Journal of Applied Polymer Science

Cationic hybrids from poly(N,N-dimethylaminoethyl methacrylate) covalently crosslinked with chloroalkyl silicone derivatives effective in binding anionic dyes

Maria Marinela Lazar, Cristian-Dragos Varganici, Maria Cazacu, Ecaterina Stela Dragan
"Petru Poni" Institute of Macromolecular Chemistry, Grigore Ghica Voda Alley 41A, Iasi, 700487, Romania
Correspondence to: E. S. Dragan (E-mail: sdragan@icmpp.ro)

ABSTRACT: The synthesis and characterization of some novel ionic organic/inorganic hybrids containing quaternary ammonium salt groups in the side chain, built on the basis of poly(N,N-dimethylaminoethyl methacrylate), as an organic component and cation provider, and chloroalkyl-functionalized silicone derivatives as crosslinkers and anion generators, are reported in this work. The resulted structures were investigated using Fourier transform infrared spectroscopy, differential scanning calorimetry, thermogravimetric analysis, and energy dispersive X-ray spectroscopy. The swelling behavior of the ionic hybrids in water as a function of pH as well as the water vapor sorption capacity in dynamic regime was also studied. The cationic hybrids have a higher swelling capacity at pH 2 compared with deionized water (pH 6) due to the presence of tertiary amine groups belonging to the organic compound. The ionic organic/inorganic hybrids were tested as potential sorbents for anionic species such as dyes [e.g., methyl orange (MO)]. The equilibrium sorption capacity increased with the increase of the organic component up to around 32 mg MO/g hybrid. © 2016 Wiley Periodicals, Inc. J. Appl. Polym. Sci. **2016**, *133*, 43942.

KEYWORDS: crosslinking; differential scanning calorimetry (DSC); hydrophilic polymers; structure–property relations; thermogravimetric analysis (TGA)

Received 23 March 2016; accepted 17 May 2016
DOI: 10.1002/app.43942

INTRODUCTION

Hydrogels are three-dimensional chemically and/or physically bound polymeric networks able to absorb significant amounts of water, the majority being able to modify their volume/phase in response to small alteration of the external stimuli.[1–6] Therefore, hydrogels have found widespread applications in pharmaceutical and medical domains,[7–9] in agriculture,[10] in separation processes,[11] etc. Special attention was recently given to ionic hydrogels, the presence of ionic or ionizable centers in their structure making them sensitive to a large number of external stimuli.[12–16] Specifically, poly(N,N-dimethylaminoethyl methacrylate) (PDMAEM) has dual temperature and pH response.[17–19] The applications of PDMAEM hydrogels in biomedicine, water treatment, and superabsorbent materials have been explored.[20–24] Lately, organic–inorganic hybrids have attracted a great deal of attention.[25,26] These materials can be obtained by chemical modification of the polysiloxane backbone with various organic functional groups. Among the polysiloxanes modified by the presence of hydrophilic functions in organic radicals particularly interesting and broadly known are those bearing quaternary ammonium salt (QAS) groups.[27] It is well known from literature that the polymers containing QAS groups present an excellent activity against some bacteria (*Escherichia coli*, *Staphylococcus albus*, *Aeromonas hydrophila*, and *Bacillus subtilis*, for example), have low toxicity, good cell membrane penetration properties, and environmental stability.[28] Some ionic organic/inorganic hybrid hydrogels containing QAS sequences, either in the backbone,[29] or in the side chain have been already reported by our group.[30,31]

In this study, Menshutkin reaction between poly[dimethyl-*co*-(chloromethyl)methylsiloxane]-α,ω-diol (S_1), poly[(chloromethyl) methylsiloxane]-α,ω,-diol (S_2), and (3-chloropropyl)trimethoxysilane (S_3) as novel crosslinkers and PDMAEM was used in order to obtain novel covalently crosslinked ionic hybrids bearing both tertiary amine groups in the side chain and QAS centers. Different from the hybrids prepared before,[31] where telechelic chloroalkylated siloxanes, such as 1,3-bis-(chloromethyl)-1,1,3,3-tetramethyldisiloxane, 1,3-bis(chloropropyl)-1,1,3,3-tetramethyldisiloxane, and α,ω-bis(chloromethyl)oligodimethylsiloxane were used, the silicone derivatives chosen here as crosslinkers for the same organic polymer have different structures allowing other crosslinking patterns with different effects on the behavior of the resulted materials. Thus, the S_1 is a copolymer where crosslinking centers statistically alternate with inert dimethylsiloxane units assuring a more uniform distribution of the crosslinking points. The S_2 possesses a crosslinking center at each silicon atom within backbone. As a result, a S_2 molecule

will assure a high number of crosslinking points. Their involving degree in crosslinking reactions will be limited by spatial steric hindrance only. The crosslinker S_3 is a commercial product that shows a single chloroalkyl group/molecule, but possesses three hydrolysable groups that, by hydrolysis/condensation, permit another three intra- or inter-molecular connections with similar groups. These crosslinkers are known silicone derivatives but they were used for first time in this combination and in this aim. The affinity for anionic species such as methyl orange (MO) of the novel hybrids was tested.

EXPERIMENTAL

Materials

(3-Chloropropyl)trimethoxysilane, >95%, molecular weight 198.72 g/mol, $d = 1.09$ g/mL; b.p. = 195 °C/750 mmHg, dichlorodimethylsilane, ≥99.5%, molecular weight 129.06 g/mol, $d = 1.07$ g/mL, b.p. = 70 °C, and dichloro(chloromethyl) methylsilane, 98%, molecular weight 163.51 g/mol, b.p. = 121–122 °C, $d = 1.284$ g/mL were purchased from Aldrich and used as received. DMAEM, purchased from Sigma-Aldrich, was distilled at 47 °C, at reduced pressure (about 4 mmHg), and kept at 4 °C. 2,2′-Azo-bis(isobutyronitrile) (AIBN), from Sigma-Aldrich, used as radical initiator, was purified by recrystallization three times from methanol. Sodium iodide, supplied by Fluka AG, was dried in vacuum on P_2O_5 before using. MO, from Sigma-Aldrich, was used after three times recrystallization from a 8 wt % solution in a mixed solvent of water and methanol (1:1 v/v). The solvents *n*-propanol, chloroform, petroleum ether (Chemical Company), and tetrahydrofuran (THF) (Fluka), all of analytical grade, were used without further purification.

Methods

Synthesis of Organic Component (PDMAEM). PDMAEM was synthesized by free radical polymerization in toluene, in the presence of AIBN, at a concentration of 1.2 wt % to DMAEM, 10 h, at 75 °C, under nitrogen.[32] Polymer was recovered by precipitation with petroleum ether. Polycation purification was performed by dialysis with Spectra/Por^{R}Dialysis Membrane with MWCO of 8.000 D, from Spectrum Labs. Comp., against distilled water for at least 3 days. The dilute aqueous solutions were concentrated by gentle heating under vacuum, and the polymer was recovered then by freeze drying with Martin Christ, ALPHA 1-2LD device (24 h, at −57 °C and 0.04 mbar). Finally, the polymer samples as white powder were dried in vacuum, at room temperature (~20 °C), in the presence of P_2O_5. The molar mass of PDMAEM was evaluated by GPC. GPC measurements were performed in THF + 2 wt % triethyl amine, at 35 °C, using a Polymer Laboratories GPC with two columns (PLgel 5 ηm Mixed C Agilant and PLgel 5 ηm Mixed D Agilant) equipped with PL-EMD 950 Evaporative Mass Detector. The molar mass was 25,500 g/mol, and PI 2.2. The chemical structures of silicone crosslinkers and PDMAEM used in this study are presented in Figure 1.

Synthesis of the Silicone Derivatives. S_1 with a content of (chloromethyl)methylsiloxane groups of 34.6 mol %, was prepared by co-hydrolysis of dichlorodimethylsilane with dichloro (chloromethyl)methylsilane in 1:1 molar ratio, in ethylic ether, in the presence of water, while the homopolymer S_2 was prepared by hydrolysis of dichloro(chloromethyl)methylsilane only

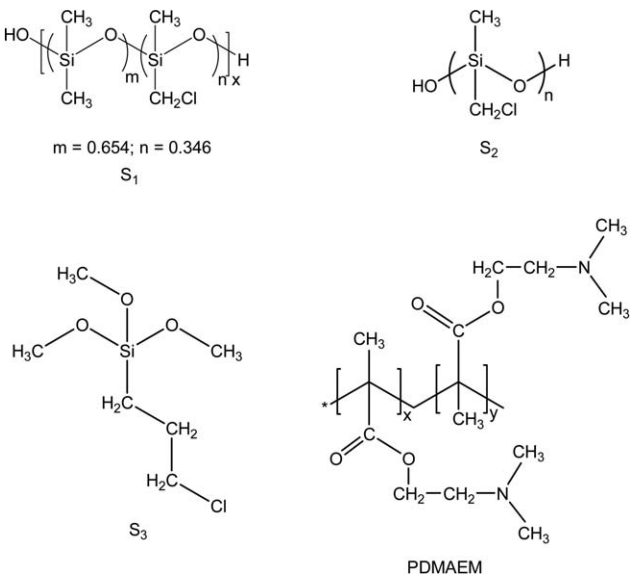

Figure 1. The chemical structures of starting reactants used in this work.

in the same conditions. Thus, both reactions were performed at room temperature under stirring for 4 h after which the mixtures were washed with a solution 5% $NaHCO_3$ and water until neutral pH. The etheric phases were dried on $CaCl_2$ and then, the ether was removed by distillation. The remained oils, consisting in mixtures of cyclic and linear oligomers, were equilibrated by mixing with 2.5 wt % sulfonic resin, Purolite CT-175, for 10 h, at 90 °C. The catalyst was removed by filtration, while the filtrates were evaporated at 150 °C/5 mmHg. The structures of the hydrolysis-equilibration products were confirmed by ^{1}H NMR spectroscopy (Figure 2). The procedure is adapted from that reported in ref. 33 except the used equilibration catalyst, trifluoromethanesulfonic acid, which in our case was replaced with an ion exchanger with sulfonic acid groups. We still have used this procedure previously.[34,35]

The composition of the copolymer S_1 was estimated on the basis of the intensity of the peak at 2.75 ppm assigned to Cl—CH_2—Si—O— protons and that at 0.071 ppm assigned to (CH_3)$_2$Si—O— protons (Figure 2 up). Molecular weights of the two polymeric crosslinkers as estimated by GPC were: S_1, $M_n = 47{,}000$, $I = 2.0$, while for S_2, $M_n = 1800$, $I = 1.6$ by using chloroform as eluent.

Synthesis of Ionic Organic/Inorganic Hybrids. The silicone derivative and PDMAEM, in different proportions, were dissolved in *n*-propanol, chloroform or THF. NaI in a molar ratio of 0.5:1, related to the chlorine content, was added as catalyst, as is specified in Table I.

The replacement of chlorine with more reactive iodine in the C—Cl group occurs in this case. The mixture was refluxed on a thermosetting bath in a flask equipped with magnetic stirrer and reflux condenser. The reaction time varied between 16 and 65 h. The reaction mixture was slowly poured on a Teflon sheet to assure the solvent evaporation at room temperature. The ionic hybrids thus obtained were removed from the sheet and maintained in vacuum at 50 °C about 24 h. All ionic hybrids

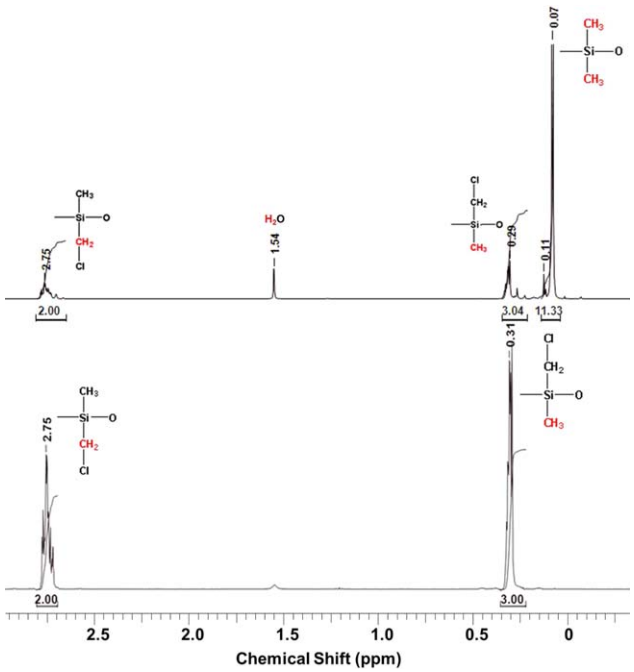

Figure 2. ^{1}H-NMR spectra for S_1 (up) and S_2 (down) recorded in $CHCl_3$ at room temperature. [Color figure can be viewed in the online issue, which is available at wileyonlinelibrary.com.]

were purified by immersion in acetone for 24 h, and then, repeatedly, washed with distilled water until the neutral pH, and finally, allowed to dry in vacuum at 50 °C for 48 h.

The reaction conditions for the synthesis of ionic hybrids are presented in Table I. The code of ionic hybrid samples listed in Table I has been abbreviated as follows: SHX:Y, where S: S_1, S_2, and S_3 representing the silicone containing component, H denotes the hybrid network, and X:Y show the weight ratio between components. The experimental and calculated values for carbon, silicon, nitrogen, chlorine, iodide, and the weight ratios (C/Si and N/Si, respectively), are presented in Table II.

Characterization of Ionic Hybrids

FTIR. The structure of all ionic hybrids was investigated by FTIR spectroscopy. The dried samples were first frozen in liquid nitrogen, and then ground in a mortar to get the samples as powder. FTIR spectra were recorded with a Bruker Vertex FTIR spectrometer, a resolution of 2 cm^{-1}, in the range 4000–400 cm^{-1} by KBr pellet technique, the amount of the sample being about 5 mg in each pellet.

^{1}H-NMR. ^{1}H-NMR spectra have been recorded on ^{1}H-NMR spectrometer of 400 MHz, Bruker Avance DRX 400, in $CDCl_3$, at room temperature. The chemical shifts are reported as δ values (ppm), referenced to the solvent residual peak (7.26 ppm).

Water Uptake. The ionic hybrids were dried in vacuum, at room temperature, in the presence of P_2O_5 and used to determine their swelling capacity. The swelling measurements were performed in distilled water with pH = 6 and in HCl aqueous solution with pH = 2, respectively, when each sample was kept in selected medium until the equilibrium swollen state was reached. The preliminary tests showed that the time necessary to attain the equilibrium swollen state was maximum 48 h. The swelling was studied using conventional gravimetric procedure. Swollen hybrids were weighed by an electronic balance after wiping the excess surface liquid by filter paper. The water uptake (W) (g/g) was defined by eq. (1):

$$W = \frac{(W_t - W_d)}{W_d} \quad (1)$$

where W_d is the weight (g) of the dried sample, and W_t is the weight (g) of the swollen sample at time t. The measurements were performed three times.

Thermogravimetric Analysis (TGA). TGA experiments were conducted on a STA 449 F1 Jupiter device (Netzsch, Germany). Samples were heated in alumina crucibles in nitrogen atmosphere at a flow rate of 50 mL/min. A heating rate of 10 °C/min was applied.

Differential Scanning Calorimetry (DSC). DSC measurements were conducted on a DSC 200 F3 Maia device (Netzsch, Germany). A mass of 10 mg of each sample was heated in pierced and sealed aluminum crucibles in nitrogen atmosphere at a flow rate of 50 mL/min and a heating rate of 10 °C/min. The device was calibrated with five different high purity metals (In, Sn, Bi, Zn, and Hg) according to standard procedures recommended by the manufacturer and the scientific literature.[36] After DSC materials measurements were completed, peak areas (ΔH) could be expressed in joules per mass unit (J/g), rather than μV·s/mg, due to the previous temperature and sensitivity calibration. Experiments baseline was obtained after calibration by scanning

Table I. Reaction Conditions for the Synthesis of the PDMAEM/Silicone hybrids

		PDMAEM/silicone			
Sample code	Silicone	Weight ratio	Molar ratio	Catalyst	Molar ratio catalyst/chlorine
S_1H2:1	S_1	2:1	1:0.36	NaI	0.5:1
S_1H1:2	S_1	1:2	1:1.4	NaI	0.5:1
S_2H2:1	S_2	2:1	1:0.75	NaI	0.5:1
S_2H1:2	S_2	1:2	1:3	NaI	0.5:1
S_3H1:1	S_3	1:1	1:0.79	NaI	0.5:1
S_3H2:1	S_3	2:1	1:0.42	NaI	0.5:1
S_3H1:2	S_3	1:2	1:1.59	NaI	0.5:1

Table II. Elemental Analysis Found by EDX and Calculated Values for the Ionic Hybrids

Sample	Element, %, found/(calculated)					Weight ratio, found/(calculated)	
	C	Si	N	Cl	I	C/Si	N/Si
$S_1H2:1$	59.77 ± 0.34 (54.01)	5.47 ± 0.45 (7)	6.25 ± 0.3 (7)	5.18 ± 0.4 (3.07)	—	11.02 ± 0.96 (7.71)	1.16 ± 0.16 (1)
$S_1H1:2$	47.71 ± 1.1 (43.78)	16.52 ± 1.16 (17.03)	3.24 ± 0.67 (4.26)	12.89 ± 1.64 (7.47)	—	2.91 ± 0.26 (2.57)	0.2 ± 0.05 (0.25)
$S_2H2:1$	50.64 ± 0.04 (51.12)	8.04 ± 0.37 (6.63)	4.46 ± 0.13 (6.63)	7.57 ± 0.82 (8.40)	12.18 ± 0.5	6.32 ± 0.3 (7.71)	0.55 ± 0.01 (1)
$S_2H1:2$	30.22 ± 0.1 (38.51)	19.28 ± 0.15 (14.97)	2.35 ± 0.04 (3.74)	8.84 ± 0.14 (18.98)	21.38 ± 0.61	1.57 ± 0.02 (2.57)	0.12 ± 0.01 (0.25)
$S_3H1:1$	52.46 ± 3.04 (47.26)	4.28 ± 0.46 (7.88)	1.89 ± 0.28 (3.94)	3.69 ± 0.41 (9.99)	20.54 ± 1.85	12.49 ± 2.04 (6)	0.46 ± 0.12 (0.5)
$S_3H2:1$	54.65 ± 0.44 (51.51)	4.88 ± 0.47 (5.46)	4.96 ± 0.24 (5.46)	5.04 ± 0.28 (6.93)	13.22 ± 1.06	11.32 ± 1.17 (9.43)	1.02 ± 0.05 (1)
$S_3H1:2$	41.3 ± 0.28 (43.32)	9.76 ± 1.38 (10.11)	3.55 ± 0.41 (2.53)	5.68 ± 0.5 (12.82)	21.39 ± 1.28	4.32 ± 0.64 (4.28)	0.38 ± 0.1 (0.25)

the corresponding temperature range with an empty pan and the temperature against heat flow, in mW/mg, was recorded afterward during the measurements of the studies structures.

Dynamic Vapor Sorption Analysis (DVS). Sorption–desorption isotherms were registered with fully automated gravimetric analyzer IGAsorp produced by Hiden Analytical, Warrington (United Kingdom). The weight change was measured with an ultrasensitive microbalance, system measurements being fully automated and controlled by a IGASORP Windows™ based software package. The samples were dried at 25 °C in flowing nitrogen (250 mL/min) until the equilibrium was reached [relative humidity (RH) < 1%]. Then, RH was gradually increased from 0 to 90% and the sorption curves were registered. The vapor pressure was stepwise increased in 10% humidity steps, with a pre-established equilibrium time between 100 and 110 min (minimum time and time out, respectively) for each of them. The cycle was ended by decreasing the vapor pressure in steps to obtain also the desorption isotherms. To evaluate Brunauer–Emmett–Teller (BET) surface, a program with 5% humidity steps between 0 and 40% RH and 10% humidity steps between 40 and 90% RH was used. For desorption, 10% humidity steps were used for the entire humidity range.

Energy Dispersive X-ray Spectroscopy (EDX). Elemental composition was determined with Environmental Scanning Electron Microscope (ESEM) type Quanta 200 having coupled an energy dispersive X-ray spectroscopy (EDX). The EDX detector is a solid state device designed to detect X-rays and convert their energy into electrical charge. This charge becomes the signal which when processed then identifies the X-ray energy, and hence its elemental source. The X-ray in its interaction with solids gives up its energy and produces electrical charge carriers in the solid. A solid state detector can collect this charge. The EDX detector used is the Si detector—EDX silicon-drift detector enables rapid determination of elemental compositions and acquisition of compositional maps. Samples are imaged at 10 mm WD (working distance), which is the stage eucentric position and the collection point of the EDX detector. It is used in conjunction with the LFD detector. LFD: Large Field Detector Accelerating Voltage: 20 kV; Low vacuum mode, uncoated samples.

Sorption of MO onto the Hybrids. In acidic condition, the tertiary amine groups of PDMAEM can be protonated. For this purpose, the hybrids were kept in aqueous solution of HCl at pH 2 until the equilibrium swollen state was reached (48 h), at room temperature. Then, the hybrids were quickly washed twice with distilled water, and twice with methanol for 2 h. Finally, the hybrids were dried in vacuum, at room temperature in the presence of P_2O_5 and used to determine their sorption capacity for MO. Tests of the sorption ability of the cationic hybrids against MO were performed as follows. About 5 mL of MO aqueous solution with a concentration of $10^{-4}M$ were added to about 5 mg of hybrid, under magnetic stirring, and the stirring went on 24 h, at room temperature (about 24 °C). About 2 mL of each mixture were centrifuged and the concentration of the dye in supernatant was measured by Specord 200 Plus

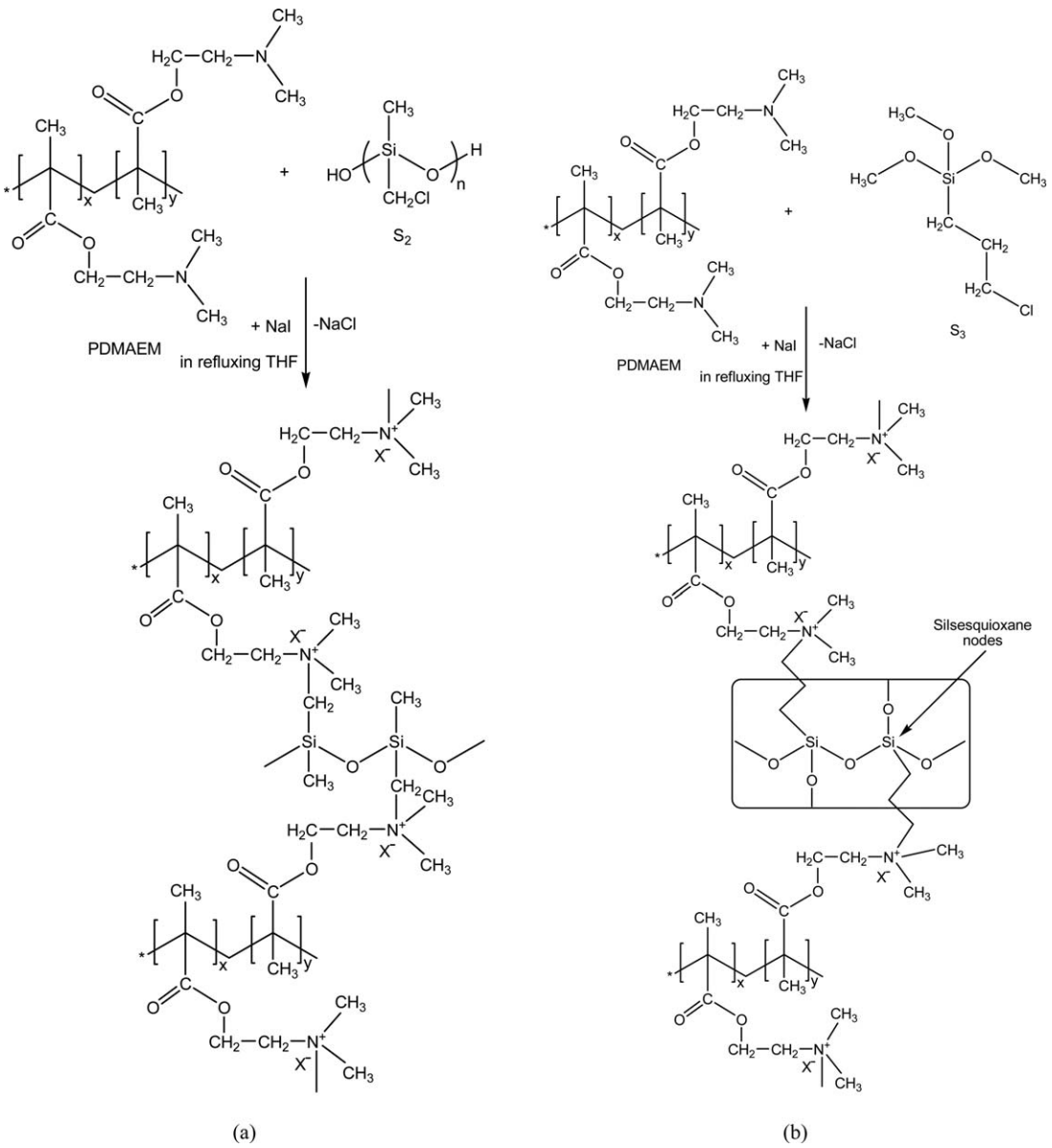

Figure 3. Schematic representation of the formation the ionic hybrids obtained with: (a) S_2 and (b) S_3 as crosslinkers.

Spectrophotometer (AnalytikJena), and the sorption capacity, q_e in mg/g, was evaluated with eq. (2):

$$q_e = \frac{(C_0 - C_e)V}{m} \quad (2)$$

where C_0 and C_e are the concentrations of the dye in aqueous solution (mg/L) before and after the interaction with the ionic hybrids, respectively, V is the volume of the dye aqueous solution (L), and m is the amount of the dried ionic hybrids (g).

RESULTS AND DISCUSSION

Formation of Ionic Hybrids

Due to the particularity of the siloxane bond and to the presence of methylsiloxane group, these crosslinkers constitute the flexible and hydrophobe part of the resulted materials besides the rigid and polar organic part consisting of PDMAEM. Thus, the resulted material will be amphiphilic. The Menshutkin reaction between silicone based crosslinkers (S_1, S_2, and S_3) and PDMAEM was used to obtain covalently crosslinked ionic hybrids containing QAS sequences in the crosslinking bridges. The crosslinking degree and the type of the functional groups of the ionic hybrids were established by the feed molar ratio between the reactive functional groups of the PDMAEM and the silicone derivatives functionalized with chloroalkyl groups (Table I and Figures 1 and 3).

As can be observed from Figure 3, the Menshutkin reaction led to the generation of positive charges by the reaction between the tertiary amine groups from the side chains of PDMAEM and the chloroalkyl functional groups from the S_2 and S_3 silicone crosslinkers (an SN_2 reaction). The reaction between S_1 and PDMAEM is similar to the one presented in Figure 3(a). It is known that for alkyl halides, the reactivity increases as the volume of the halogen atom increases in the following order:

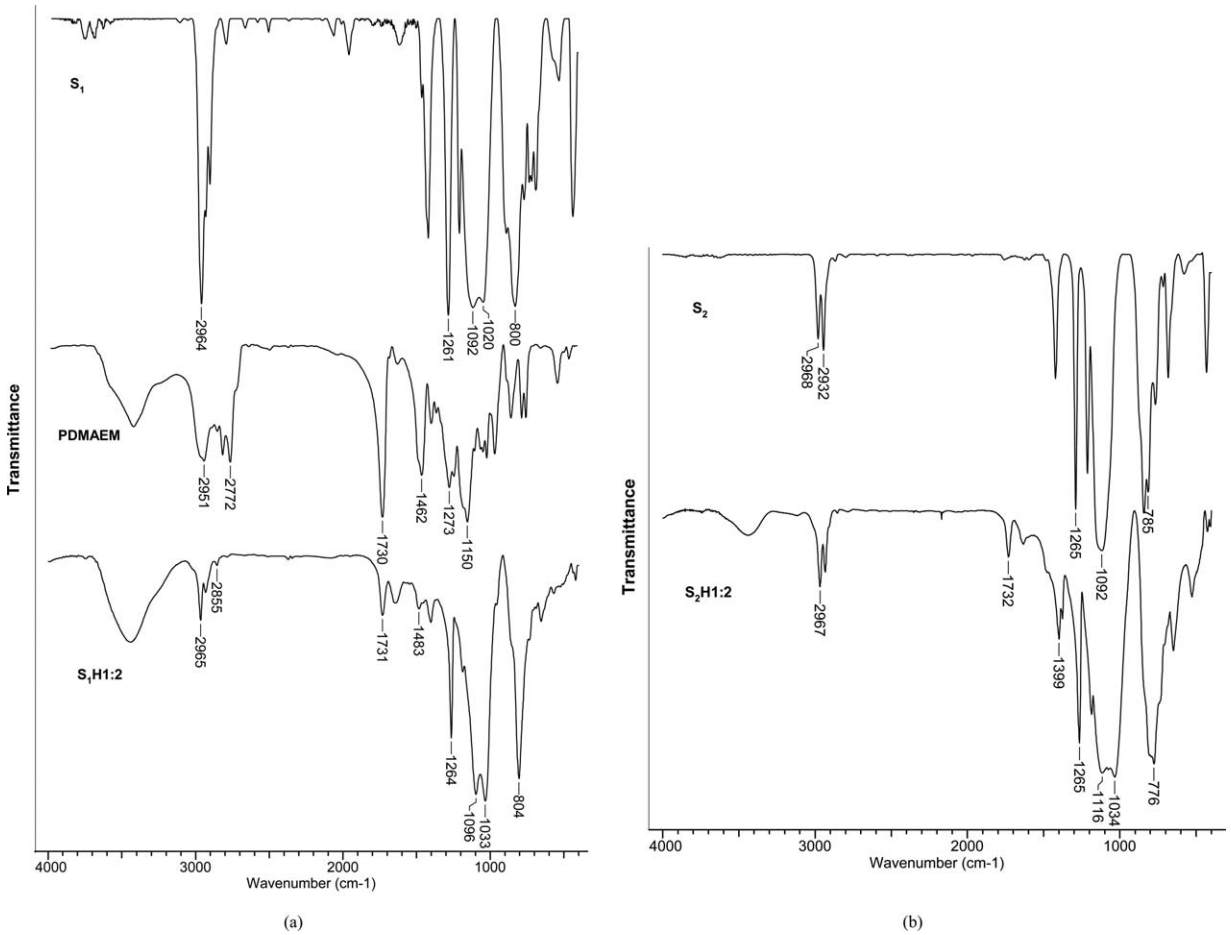

Figure 4. FTIR spectra of the starting reactants and some ionic hybrids: (a) S_1, PDMAEM and $S_1H1:2$; (b) S_2 and $S_2H1:2$; (c) S_3 and $S_3H1:1$.

I > Br > Cl > F. This is due to the fact that iodoalkyl groups have a much higher reactivity toward the tertiary amine, compared with chloroalkyl groups. Therefore, the chloroalkyl groups from the silicone derivatives were converted into an iodoalkyl group by halogen substitution with NaI. As can be observed from Table II, when S_1 was used as a crosslinker in the reaction with PDMAEM, at a molar ratio between functional groups of 1:1.4 ($S_1H1:2$), silicon and chlorine contents increased, compared with the sample having the tertiary amine groups in excess ($S_1H2:1$). In the case of the crosslinker S_2 ($S_2H1:2$), prepared at a molar ratio between reactive functional groups of 1:3 and a higher concentration of the reactant, in the presence of NaI (0.5:1), high amount of silicon and chlorine were incorporated in the hybrid. Increasing the molar ratio between tertiary amine and chlorine up to 1:0.75, determined an increase of nitrogen content in hybrid, as expected ($S_2H2:1$). The silicone crosslinker S_3 was more effective in the reaction with PDMAEM, a molar ratio between reactive functional groups of 1:1.59 ($S_3H1:2$) leading to the increase of the silicon and chlorine contents (Table II). In the case of this crosslinker, concomitantly with the Menshutkin reaction, under the environmental humidity and in the presence of ammonium groups belonging to PDMAEM, a hydrolysis/condensation reaction of the easy hydrolysable Si-OCH_3 groups occurs with the formation of the silsesquioxane domains that in fact are the crosslinking nodes. The excess of tertiary amine groups would lead to an increase of the pH responsivity of the hybrid ($S_3H2:1$), as the swelling behavior will demonstrate. Table II shows a satisfactory agreement between the found and calculated values for carbon contents. From Table II, it can be seen that found and calculated values for the weight ratio N/Si are higher when the hybrid samples present an excess of tertiary amine groups.

Spectral Characterization

FTIR spectroscopy was used to identify any changes in the structure of the covalently crosslinked ionic hybrids compared with that of the starting PDMAEM and silicone crosslinkers. The silicone structure and the synthesis conditions may influence the intensity of the characteristic bands for silicone derivative. The FTIR spectra of crosslinkers, PDMAEM and some ionic hybrids are shown in Figure 4(a–c), respectively.

In the FTIR spectrum of $S_1H1:2$ ionic hybrid, the presence of PDMAEM is supported by the peaks located at 1731 cm^{-1} attributed to the stretching vibration of C═O in ester group, the peaks from 2965 cm^{-1}, 2855 cm^{-1}, and 1483 cm^{-1} are assigned to the stretching of C—H from aliphatic (CH_3, CH_2) groups. The band at 1150 cm^{-1} assigned to C—N stretching in tertiary amine groups found in PDMAEM spectrum, was not visible in the hybrid spectrum, being covered by characteristic bands of the Si—O—Si bonds. Moreover, the characteristic

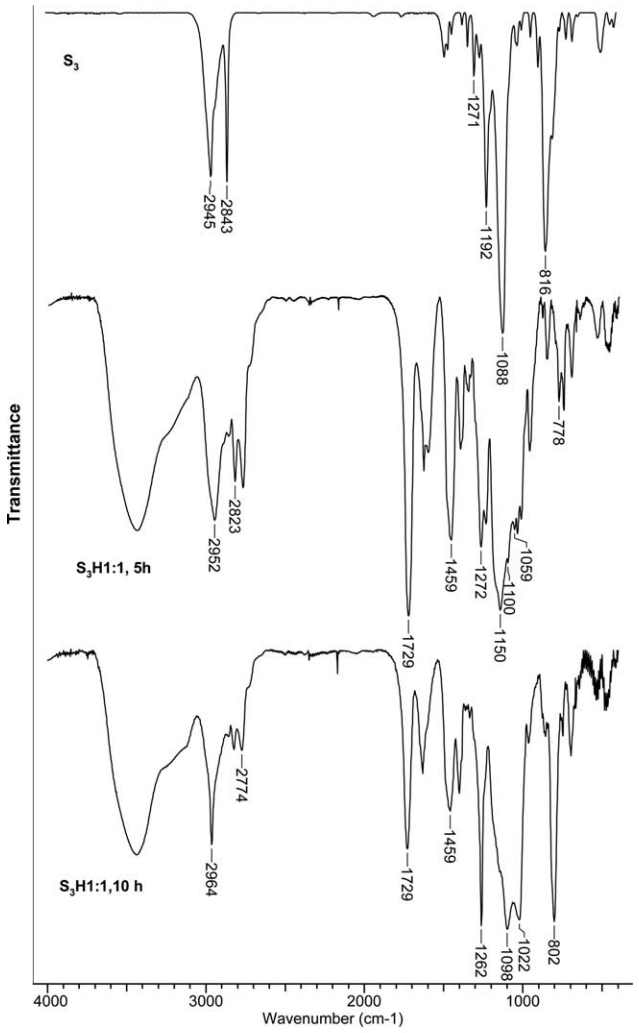

(c)

Figure 4. (Continued).

bands of the inorganic component can be observed at: 804 cm^{-1} and 1264 cm^{-1} assigned to the deformation of Si—C bond in Si—CH_3 groups, as well as in the region 1033–1096 cm^{-1} attributed to the Si—O—Si bond. In the spectrum of the hybrid obtained with silicone crosslinker S_2, the presence of PDMAEM is confirmed by the bands at 1732 cm^{-1}, and by the peak at 1150 cm^{-1}, attributed to C—N stretching in tertiary amine, shifted to about 1116 cm^{-1} in hybrid. The presence of crosslinking agent S_2, is supported by the bands located at 776 cm^{-1} and 1265 cm^{-1} attributed to C—Si bond in Si—CH_3 groups, and by the peak at 1034 cm^{-1} assigned to Si—O—Si bonds. The crosslinker S_3, being an organotrimethoxysilane, that does not contain Si—O—Si group, shows in its IR spectrum a sharp and intense band at 1088 cm^{-1} assigned to the stretching of Si—O—C bond besides to bands at 816 and 1192 cm^{-1} corresponding to Si—C bond and the bands at 2843 and 2945 cm^{-1} due to C—H vibration from Si—OCH_3 and Si—$(CH_2)_3$ groups, respectively. The FTIR spectrum of the product resulting from the reaction of S_3 with PDMAEM isolated after 5 h is dominated by the characteristic absorption bands of the latter (1150, 1272, and 1729 cm^{-1}), while the peak at 1059 cm^{-1} is attributed to the newly formed Si—O—Si bonds as a result of hydrolysis/condensation reaction of easy hydrolizable Si—O—CH_3 groups from the silane derivative. The band at 1088 cm^{-1} in the spectrum of the crosslinker S_3 is shifted at a higher frequency, at 1100 cm^{-1} in the spectrum of the ionic hybrid being assigned to the unhydrolyzed Si—O—C groups. After 10 h, it is obvious the evolution of crosslinking process by the emergence of a strong, broad and split band at 1022–1098 cm^{-1} characteristic for Si—O—Si bond from the formed silsesquioxane domains.

Water Uptake as a Function of pH

The swelling behavior of a polymer network depends on a number of factors, like hydrophilic/hydrophobic balance of the network, the presence of ionic or ionizable groups and the crosslinking extent of the network.[37] The swelling behavior as a function of pH at 25 °C for the ionic hybrids are shown in Table III and Figure 5.

As can be observed, the hybrids containing amine groups in the highest excess toward chloroalkyl groups (1:0.36 and 1:0.42 in $S_1H2:1$ and $S_3H2:1$, respectively) seem to be the most hydrophilic and this characteristic is enhanced with decreasing pH in all cases. According to Table III, the highest values for *W* were obtained for samples crosslinked with crosslinker S_1 that consists of a siloxane copolymer containing 34.6 mol % of (chloromethyl)methylsiloxane groups, the remaining being dimethylsiloxane units which do not participate in crosslinking. Therefore, a higher number of free amine groups will remain. In the samples crosslinked with S_2, containing only (chloromethyl)methylsiloxane groups in molecule, the number of free amino groups will be lower and, as a result will have lower hydrophilicity. For samples cured with S_3, although it would be expected to increase hydrophilicity, *W* capacity is lower, likely because of higher crosslinking degree achieved both through ionic but especially by covalent bonds formed by condensation of Si—OH groups. The content of PDMAEM influenced the W values, PDMAEM being a weak polycation, its affinity for water increasing with the increase of the degree of protonation of the tertiary amine groups. In the acidic medium, the protonation of the amine groups leads to the repulsion in the polymer chains, thus allowing more water to penetrate the hybrid network. In pure water (pH 6), the repulsion between cationic groups decreased and, therefore, the amount of water in the hybrid decreased accordingly.[2]

Table III. Water Uptake (*W*) of the Ionic Hybrids at 25 °C

Sample code	Silicone	*W*, g/g		*W* (pH 2)/ *W* (pH 6)
		pH 6	pH 2	
$S_1H2:1$	S_1	4.10	17.89	4.36
$S_1H1:2$		6.71	8.27	1.23
$S_2H2:1$	S_2	3.67	5.80	1.58
$S_2H1:2$		2.70	4.74	1.76
$S_3H1:1$	S_3	1.81	1.74	0.96
$S_3H2:1$		2.55	5.80	2.27
$S_3H1:2$		1.60	1.82	1.14

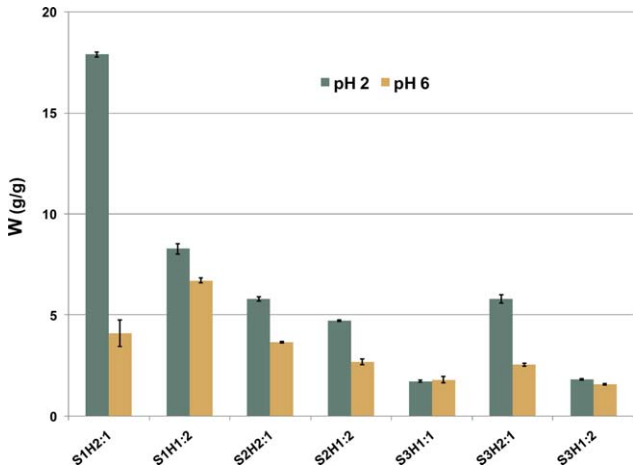

Figure 5. Comparative water uptake values (W) of the ionic hybrids at 25 °C at two different pH values; the results are represented as means ± standard deviation ($n = 3$). [Color figure can be viewed in the online issue, which is available at wileyonlinelibrary.com.]

TGA and DSC Measurements

The thermal stability of the ionic organic/inorganic hybrids was evaluated by TGA performed in inert atmosphere. The thermogravimetric, TG, curves and the differential weight loss, DTG, curves, of the ionic hybrid are presented in Figure 6.

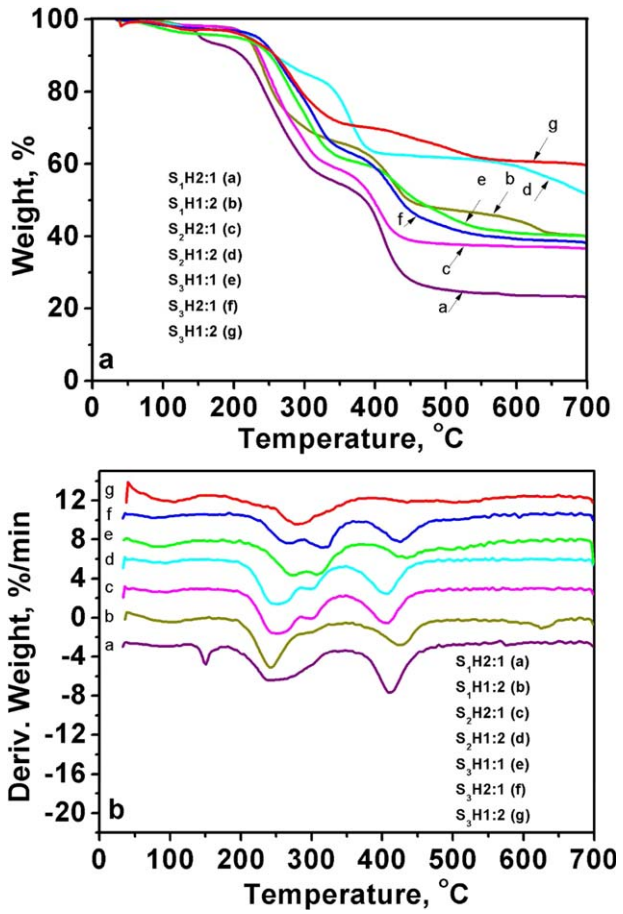

Figure 6. Thermogravimetric analysis results of ionic organic/inorganic hybrids: (a) TG curves; (b) DTG curves. [Color figure can be viewed in the online issue, which is available at wileyonlinelibrary.com.]

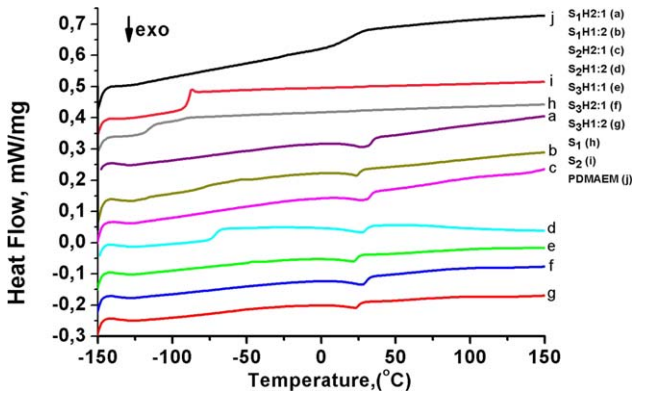

Figure 7. DSC thermograms of ionic hybrids, crosslinkers (S_1, S_2) and initial non-crosslinked polymer (PDMAEM). [Color figure can be viewed in the online issue, which is available at wileyonlinelibrary.com.]

As Figure 6 shows the thermal degradation runs in four, five, or six stages, indicating a different degradation pathway of hybrids as a function of the main parameters varied in the synthesis and the crosslinking agent structure. From Figure 6, one may observe that the hybrids exhibit decreasing weight from the beginning, due to the hygroscopic nature of the highly hydrophilic quaternary ammonium centers and the implied solvents. In general, this may lead to thermal history in more than one stage, with a relatively high humidity loss.[38] The thermograms of the studied compounds may obviously be divided into two sequences. The first part consists of the dehydration and QAS groups decomposition, ranging through temperature values up to 300 °C.[27] The second sequence corresponds to the silicone polymer chains decomposition, around or higher than 300 °C.[39] It is known that, due to its partially ionic character, the Si—O bond possesses high bond dissociation energy values.[40] Due to this aspect, the increase of the siloxane chain lengths improves thermal stability.[41] In this sense, it was observed that the residual content increased with increasing ratio of silicone moieties, thus depending on their molecular weight, the values found being as follows: 22.88, 39.81, 36.3, 51.26, 39.62, 37.95, and 59.4%, for $S_1H2{:}1$, $S_1H1{:}2$, $S_2H2{:}1$, $S_2H1{:}2$, $S_3H1{:}1$, $S_3H2{:}1$, and $S_3H1{:}2$, respectively. The residual mass that remained at 700 °C is generated by the Si—O bond presence. That is the reason why higher molecular weights of the crosslinkers lead to increasing SiO_2 residue mass.[27]

The determination of the glass transition temperature, T_g, represents a very useful tool in the evaluation of the miscibility of two polymers. Figure 7 and Table IV show the second heating runs and DSC data of the studied structures. The generally weak T_g intensities compared with those of the pure comprising components are due to curing and they may slightly vary depending on crosslinking degree. Higher crosslinking densities may lead to very less intense and unobservable T_g values or even to their complete disappearance, as further demonstrated.

By analyzing Figure 7 and Table IV one may observe that, besides the initial polymer (PDMAEM) and crosslinkers (S_1,

Table IV. Characteristics of Ionic Organic/Inorganic Hybrids, Crosslinkers (S_1, S_2) and Initial Non-Crosslinked Polymer (PDMAEM) Corresponding to the DSC Thermograms

Sample	T_g, °C	T_{cp} °C	ΔH, J/g
S_1H2:1	-	27	−2.3
S_1H1:2	−76	23	−0.92
S_2H2:1	-	27	−2.03
S_2H1:2	−71	28	−1.42
S_3H1:1	-	21	−0.96
S_3H2:1	-	27	−1.55
S_3H1:2	-	23	−0.7
S_1	−116	-	-
S_2	−89	-	-
PDMAEM	19	-	-

S_2), only structures containing silicon crosslinkers in excess against tertiary amine groups and of higher molar masses exhibited T_gs. T_g values at −76 °C and −71 °C for the samples S_1H1:2 and S_2H1:2 are assigned to methyl(chloromethyl)siloxane units, that are in the highest contents in these hybrids. The T_g value increases with increasing of the chloromethyl groups content, as in the case of sample S_2H1:2 in which the (chloromethyl)methylsiloxane homopolymer was used as crosslinker in 3:1 molar ratio related to the organic component. The T_g value is influenced by chain length and flexibility. The initial non-crosslinked polymer (PDMAEM) exhibited a T_g value at 19 °C, the same value being reported in the literature.[42] Since the S_3 crosslinker is not a polymer, it did not exhibit a T_g. Siloxane entities from S_1 and S_2 crosslinkers exhibit free —Si—O—Si— linkage rotation (bond angle 130.5°), which endows the siloxane bond with low cohesive energy, thus increasing its flexibilty, even at low temperature values.[43] The higher the siloxane chain length, the lower the T_g value. This explains the low T_g values of crosslinkers S_1 (−116 °C), S_2 (−89 °C) and of the samples crosslinked with S_2 (−71 °C) and with S_1 (−76 °C) in 1:1.4 molar ratio and 1:3, respectively. The absence or very weak unobservable detection of T_g for structures crosslinked with S_3 is due to the increased rigidity imposed by the high crosslinking degree achieved through ionic and covalent bonds formed by of Si—OH groups condensation, confirmed through the swelling behavior results. Another explanation resides in the fact that the presence of a single T_g is an indication of a good miscibility of the crosslinked polymer networks, generated by a forced phase compatibilization, leading to a synergism of the properties of the individual components in the networks.[44] Also, the presence of a single T_g for the copolymer crosslinker S_1 (−116 °C) confirms its successful synthesis. The two discussed T_g values (−71 °C and −76 °C) are significantly higher than that of pure poly(dimethylsiloxane) [PDMS (−125 °C)], due to a slightly rigid character imposed by the presence of chloromethyl moieties from alternating silicon atoms. Occurrence of the phase transition characteristic to the lower critical solution temperature (LCST) resides in establishment of hydrogen bonds between polymer chains.[45] Hydrogen bond cleavage occurs when heating above the cloud point temperature (T_{cp}), leading to hydrophobic interactions increase between polymer chains.[46] All structures exhibit a weak exothermic transition in the range 0–50 °C. The exothermic peak temperatures correspond to the T_{cp}, the transition being attributed to a thermo-induced structural packing phenomenon.[47]

Water Vapors Sorption–Desorption Isotherms

DVS is a rapid method for characterization of sorption/desorption isotherms of various materials. The sorption and desorption isotherms performed at 25 °C for the prepared hybrids are presented in Figure 8.

The average pore size was estimated based on the desorption branch assuming cylindrical pore geometry using eq. (3).[48,49]

$$r_{pm} = \frac{2 \cdot n}{100 \cdot \rho_a \cdot A} \quad (3)$$

where: r_{pm} is the average pore size, nm, A is the BET surface area, m^2/g,[48] n is the percentage uptake of water, and ρ_a is the adsorbed phase density.

Sorption–desorption curves correspond to the type IV isotherms, describing the adsorption behavior of mesoporous materials with pore condensation together with hysteresis loop between adsorption and desorption branch. The isotherms present type H_2 hysteresis loop, characteristic for more irregular array of pore shape. In Table V are listed the data obtained from the sorption and desorption isotherms. The sorption capacities of ionic hybrids are different and can be explained by their structural diversity. As can be seen from Table V, the values of the sorption capacity increased in the following order: S_2H2:1 > S_1H2:1 > S_1H1:2 > S_3H1:2 > S_3H2:1 > S_3H1:1 > S_2H1:2, S_1H2:1 > S_1H1:2 > S_3H1:2 > S_3H2:1 > S_3H1:1 > S_2H1:2, whereas the order of the BET surface area values was different: S_1H1:2 > S_2H2:1 > S_3H1:1 > S_1H2:1> S_3H2:1 > S_3H1:2 > S_2H1:2. The nature of the polar groups, available in ionic hybrids structure, can determine the difference between surface area and the order of water sorption capacity.

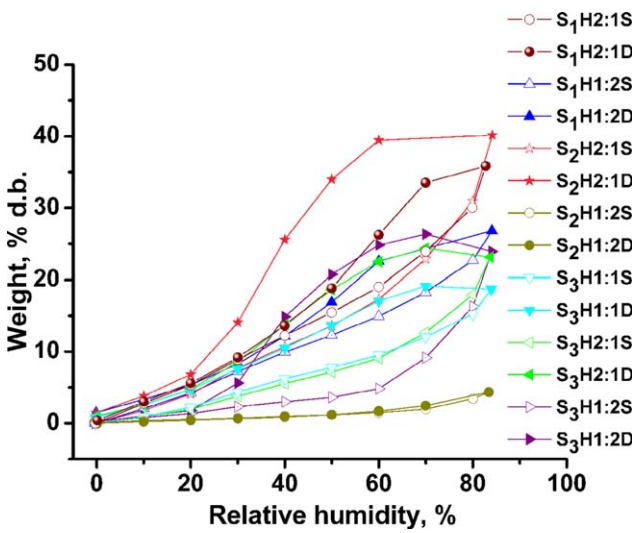

Figure 8. Sorption and desorption isotherms for ionic hybrids determined by DVS method. [Color figure can be viewed in the online issue, which is available at wileyonlinelibrary.com.]

Table V. The Main Surface Parameters Evaluated Based on Sorption Isotherms

Sample	Sorption capacity, %	Average pore size, nm	BET data[a] Area, m^2/g	Monolayer, g/g
$S_1H2:1$	35.84	1.66	434	0.1237
$S_1H1:2$	26.81	0.63	855	0.240
$S_2H2:1$	40.15	1.30	618	0.176
$S_2H1:2$	4.35	3.49	25	0.007
$S_3H1:1$	19.13	0.74	516	0.147
$S_3H2:1$	24.37	1.56	313	0.089
$S_3H1:2$	26.32	5.80	91	0.026

[a] The range of relative humidity was 5–40%.

Sorption of MO onto Ionic Hybrids

All hybrids based on PDMAEM and the silicone derivatives were tested for their capacity to adsorb the anionic dye MO. As can be seen in Figure 9, the highest sorption capacity was found for the hybrids where the cationic polymer (PDMAEM) was the major component, that is, $S_1H2:1$, $S_2H2:1$, $S_3H2:1$, and $S_3H1:1$, the values being 27.28, 29.61, 31.6, and 28.81, mg/g, respectively.

An exception was found in the case of the hybrid $S_1H1:2$, which although has the silicone component in excess has a sorption capacity comparable with the first four samples (28.82 mg/g). This surprising behavior could be attributed to the copolymeric nature of the crosslinker S_1, where (chloromethyl)methylsiloxane groups acting as crosslinking centers statistically alternate with inert dimethylsiloxane units. This is expected to assure a more uniform distribution of the crosslinking points and porosity. According to DVS data, this sample shows the smallest value for average pore size (0.63 nm) and the highest value for BET area (855 m^2/g). Much lower sorption capacities were found in the case of the hybrids prepared with the crosslinkers S_2 and S_3 in excess, i.e. $S_2H1:2$ and $S_3H1:2$, the corresponding values of MO sorption being 8.8 and 13.31 mg/g, respectively. Thus, the sorption capacities of MO as a model dye were in good agreement with the hydrophylicity of the hybrids, the equilibrium sorption capacity decreasing with the decrease of the organic component.

Figure 9. Optical images of the ionic hybrids after the sorption of MO from an aqueous solution with a concentration of 10^{-4} M; sorbent dose: 5 mg; volume of dye solution 5 mL; temperature 24 °C; pH ~ 5.5; sample code from the left to the right: (1) $S_1H2:1$; (2) $S_1H1:2$; (3) $S_2H2:1$; (4) $S_2H1:2$; (5) $S_3H1:1$; (6) $S_3H2:1$; (7) $S_3H1:2$. [Color figure can be viewed in the online issue, which is available at wileyonlinelibrary.com.]

CONCLUSIONS

Novel ionic organic/inorganic networks containing QAS sequences in the crosslinking bridges were obtained in this study by the Menshutkin reaction of PDMAEM with silicone derivatives functionalized with chloroalkyl groups. The chemical structure of the ionic hybrids was supported by the FTIR spectra, EDX, DSC, and thermal analysis. It was found that the properties of the ionic hybrids strongly depended on the following parameters: the concentration of components and the molar ratio between reactants, the crosslinking agent structure, and the presence of a catalyst. Thus, for the ionic organic–inorganic hybrids prepared with an excess of chloroalkyl groups, the silicone and chlorine contents increased, compared with the sample having the tertiary amine groups in excess. The samples with an excess of tertiary amine groups swell at a higher level, perhaps due to the lower crosslinking degree. These novel ionic hybrids are pH sensitive materials due to the presence of tertiary amine groups besides QAS centers. DSC measurements indicated a good miscibility, due to the presence of a single T_g, and a weak exothermic transition corresponding to the T_{cp} and describing a thermo-induced structural packing phenomenon. TGA experiments indicated two sequences of thermal decomposition corresponding to dehydration with QAS groups decomposition and silicone polymer chains decomposition. The surface areas were estimated on the basis of the BET sorption isotherms. The presence of QAS centers and of the tertiary amine groups endow the novel ionic hybrids with sorption properties for anionic species, the MO being used as a model in this work.

ACKNOWLEDGMENTS

This work was supported by a grant of the Romanian National Authority for Scientific Research, CNCSIS–UEFISCDI, project number PN–II–ID–PCE–2011–3–0300.

REFERENCES

1. Hoare, T. R.; Kohane, D. S. *Polymer* **2008**, *49*, 1993.
2. Dragan, E. S.; Perju, M. M. *Soft Matter* **2010**, *8*, 49.
3. Zhao, Y.; Liu, W.; Yang, X.; Xu, H. *J. Appl. Polym. Sci.* **2008**, *110*, 2234.
4. Wang, Y.; Dong, A.; Yuan, Z.; Chen, D. *Colloids Surf. A* **2012**, *415*, 68.
5. Lim, S. L.; Tang, W. N. H.; Ooi, C. W.; Chan, E. S.; Tey, B. T. *J. Appl. Polym. Sci.* **2016**, *133*, DOI: 10.1002/app.43515.
6. Dragan, E. S.; Perju, M. M.; Dinu, M. V. *Carbohydr. Polym.* **2012**, *88*, 270.
7. Faccia, P. A.; Pardini, F. M.; Amalvy, J. I. *eXPRESS Polym. Lett.* **2015**, *9*, 554.
8. Bajpai, A. K.; Shukla, S. K.; Bhanu, S.; Kankane, S. *Prog. Polym. Sci.* **2008**, *33*, 1088.
9. Gómez, M. L.; Williams, R. J. J.; Montejano, H. A.; Previtali, C. M. *eXPRESS Polym. Lett.* **2012**, *6*, 189.
10. Demitri, C.; Scalera, F.; Madaghiele, M.; Sannino, A.; Maffezzoli, A. *Int. J. Polym. Sci.* **2013**, *2013*, 1.

11. Dragan, E. S.; Lazar, M. M.; Dinu, M. V.; Doroftei, F. *Chem. Eng. J.* **2012**, *204–206*, 198.
12. Huang, Y.; Liu, M.; Wang, L.; Gao, C.; Xi, S. *React. Funct. Polym.* **2011**, *71*, 666.
13. Zhang, X.; Li, C.; Hu, Y.; Liu, R.; He, L.; Fang, S. *Polym. Int.* **2014**, *63*, 2030.
14. Richter, A.; Paschew, G.; Klatt, S.; Lienig, J.; Arndt, K.-F.; Adler, H.-J. *Sensors* **2008**, *8*, 561.
15. Cho, E. C.; Lee, J.; Cho, K. *Macromolecules* **2003**, *36*, 9929.
16. Ilmain, F.; Tanaka, T.; Kokufuta, E. *Nature* **1991**, *349*, 400.
17. Orakdogen, N. *Polym. Eng. Sci.* **2013**, *53*, 734.
18. Emileh, A.; Vasheghani-Farahani, E.; Imani, M. *Eur. Polym. J.* **2007**, *43*, 1986.
19. París, R.; Quijada-Garrido, I. *Eur. Polym. J.* **2010**, *46*, 2156.
20. Wang, L.; Liu, M.; Gao, C.; Ma, L.; Cui, D. *React. Funct. Polym.* **2010**, *70*, 159.
21. Wu, W.; Liu, J.; Cao, S.; Tan, H.; Li, J.; Xu, F.; Zhang, X. *Int. J. Pharm.* **2011**, *416*, 104.
22. Zhang, N.; Liu, M.; Shen, Y.; Chen, J.; Dai, L.; Gao, C. *J. Mater. Sci.* **2011**, *46*, 1523.
23. Wang, J.; Song, D.; Jia, S.; Shao, Z. *React. Funct. Polym.* **2014**, *81*, 8.
24. Bardajee, G. R.; Hooshyar, Z.; Zehtabi, F.; Pourjavadi, A. *Iran. Polym. J.* **2012**, *21*, 829.
25. Duraibabu, D.; Ganeshbabu, T.; Saravanan, P.; Kumar, A. S. *High Perform. Polym.* **2014**, *26*, 725.
26. Xue, Y.; Wang, L.; Shao, Y.; Yan, J.; Chen, X.; Lei, B. *Chem. Eng. J.* **2014**, *251*, 158.
27. Cui, X.; Qiao, C.; Wang, S.; Ding, Y.; Hao, C.; Li, J. *Colloid Polym. Sci.* **2015**, *293*, 1971.
28. Zhang, A.; Liu, Q.; Lei, Y.; Hong, S.; Lin, Y. *React. Funct. Polym.* **2015**, *88*, 39.
29. Dragan, S.; Cazacu, M.; Tóth, A. *J. Polym. Sci. Part A: Polym. Chem.* **2002**, *40*, 3570.
30. Cazacu, M.; Ghimici, L.; Dragan, E. S. *J. Polym. Sci. Part A: Polym. Chem.* **2004**, *42*, 3720.
31. Dragan, E. S.; Cazacu, M.; Nistor, A. *J. Polym. Sci. Part a: Polym. Chem.* **2009**, *47*, 6801.
32. Dragan, E. S.; Dinu, I. A. *Eur. Polym. J.* **2011**, *47*, 1065.
33. Sauvet, G.; Dupond, S.; Kazmierski, K.; Chojnowski, J. *J. Appl. Polym. Sci.* **2000**, *75*, 1005.
34. Alexandru, M.; Cazacu, M.; Racles, C.; Grigoras, C. *Polym. Eng. Sci.* **2011**, *51*, 78.
35. Cazacu, M.; Ioanid, A.; Ioanid, G.; Racles, C.; Vlad, A. *Appl. Organomet. Chem.* **2006**, *20*, 494.
36. Höhne, G. W. H.; Cammenga, H. K.; Eysel, W.; Gmelin, E.; Hemminger, W. *Thermochim. Acta* **1990**, *160*, 1.
37. Chen, Y.; Xiong, Y.; Peng, C.; Liu, W.; Peng, Y.; Xu, W. *J. Polym. Sci. Part B: Polym. Phys.* **2013**, *51*, 1494.
38. Kang, J.-J.; Li, W.-Y.; Lin, Y.; Li, X.-P.; Xiao, X.-R.; Fang, S.-B. *Polym. Adv. Technol.* **2004**, *15*, 61.
39. Kweon, J.-O.; Lee, Y.-K.; Noh, S.-T. *J. Polym. Sci. Part A: Polym. Chem.* **2001**, *39*, 4129.
40. Schmaucks, G.; Sonnek, G.; Wustneck, R.; Herbst, M.; Ramms, M. *Langmuir* **1992**, *8*, 1724.
41. Filippou, A. C.; Baars, B.; Chernov, O.; Lebedev, Y. N.; Schnakenburg, G. *Angew. Chem. Int. Ed.* **2014**, *53*, 565.
42. Roy, S. G.; Bauri, K.; Pal, S.; Goswami, A.; Madras, G.; De, P. *Polym. Int.* **2013**, *62*, 463.
43. Soni, S. S.; Sastry, N. V.; Aswal, V. K.; Goyal, P. S. *J. Phys. Chem. B* **2002**, *106*, 2606.
44. Varganici, C. D.; Rosu, L.; Rosu, D.; Simionescu, B. C. *Compos. Part B: Eng* **2013**, *50*, 273.
45. Yang, L.; Liu, T.; Song, K.; Wu, S.; Fan, X. *J. Appl. Polym. Sci.* **2013**, *127*, 4280.
46. Thavanesan, T.; Herbert, C.; Plamper, F. A. *Langmuir* **2014**, *30*, 5609.
47. Wagner, M.; Pietsch, C.; Kerth, A.; Traeger, A.; Schubert, U. S. *J. Polym. Sci. Part A: Polym. Chem.* **2015**, *53*, 924.
48. Brunauer, S.; Emmett, P. H.; Teller, E. *J. Am. Chem. Soc.* **1938**, *60*, 309.
49. Murray, K. L.; Seaton, N. A.; Day, M. A. *Langmuir* **1999**, *15*, 6728.